

AN ACCURATE AND ROBUST CONTACT RESOLUTION ALGORITHM FOR FINITE-DISCRETE ELEMENT MODELLING

HU CHEN^{*}, Y.X ZHANG^{*}, MENGYAN ZANG[†] AND PAUL J. HAZELL^{*}

^{*}School of Engineering and Information Technology
The University of New South Wales, Canberra, at the Australian Defence Force Academy
ACT 2600, Australia

e-mail: hu.chen@student.adfa.edu.au, www.unsw.adfa.edu.au

[†]School of Mechanical and Automotive Engineering
South China University of Technology
Guangzhou 510640, P. R. China

Key Words: *Contact resolution algorithm, Discrete element, Finite element, Hertz contact, Hierarchical searching.*

Abstract. An accurate and robust contact resolution algorithm is proposed for resolving contact problems between spherical particles (discrete elements) and finite element facets. The contact resolution is divided into three types: particle-to-facet (PTF), particle-to-edge (PTE) and particle-to-vertex (PTV). PTF has the top priority and is checked first, PTE is superior to PTV and accordingly checked ahead of the latter. The invalid contacts can be removed by means of priority definition. The algorithm is consistent and failed information can be passed down from PTF to PTE and to PTV, which makes the implementation straightforward.

1 INTRODUCTION

The combined finite-discrete element method [1] is able to take advantage of the merits of finite element and discrete element methods and meanwhile avoid their drawbacks; therefore, this method recently draws much attention and its application becomes increasingly common. It is found that this method is advantageous in the modelling with fragile material involved, such as tire-soil interaction problems [2, 3] and the case of laminated glass subjected to ballistic impact [4].

Looking at the computational modelling aspect of aforementioned problems in finite-discrete element system, one of the most critical issues is to efficiently, accurately and robustly resolve contact problems between finite element facets and spherical particles that are usually the representative geometries of discrete elements. Numerical approaches to achieve that purpose are generally comprised of two successive stages, contact detection and interaction. The former one further consists of two inherently-related stages, spatial searching and contact resolution, mainly affecting computational efficiency and robustness, respectively; while the latter, contact interaction, affects the accuracy of contact force

computation.

The aim of this work is to propose an accurate and robust contact resolution algorithm to resolve contact problems between facets and spherical particles in finite-discrete element modelling. The widely-used glued-sphere approach [5] is simple as it approximates any complicated geometry by a collection of spheres; however, it is inaccurate and computational intensive. Considering the reality that a particle may be in contact with a facet or an edge or even a vertex, Dang and Meguid [6] and Kremmer and Favier [7] proposed contact resolution algorithms for contact problems between spherical particles and triangular facets; Zang et al. [8] developed an algorithm accounting for quadrilateral facets; a more elaborate algorithm, RIGID [9], can tackle contact problems involving complex geometries. To exclude invalid contacts, Hu et al. [10] presented an robust algorithm based on barycentric coordinates of triangular facets. In present work, the contact resolution takes particle-to-facet (PTF), particle-to-edge (PTE) and particle-to-vertex (PTV) into account to robustly handle each kind of contact problems. Among them, PTF has top priority, and PTE is superior to PTV; this treatment is reasonable from the physical point of view. For any contact pairs, PTF starts firstly, and PTE would not commence until PTF is confirmed failed, and so does PTV until PTE confirmed failed as well. This hierarchical searching strategy is simple to find the edge or vertex that possibly in contact as inherent failed information can be passed down from PTF to PTE and to PTV. Because of priority definition, the invalid contacts can be correctly removed, which avoids double checks and repetitive computation of contact force. To accurately compute contact force, the Hertz contact model [11] is used.

2 CONTACT RESOLUTION

For each contact pair recorded in spatial searching stage, its uncertain contact state needs further geometrical resolution. To robustly examine contact state of each contact pair, a hierarchical searching strategy is proposed in this section. This strategy is comprised of three searching levels, i.e., PTF, PTE and PTV, and they will be detailed in this section.

2.1 PTF contact

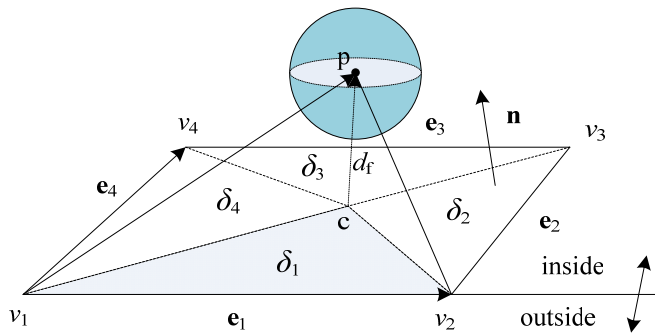


Figure 1: PTF contact checking

The PTF is first conducted to check geometrical relation between a particle and a facet by means of inside-outside approach [12]. Before doing so, the distance d_f (Figure 1) between the centre of that particle and the facet is calculated to check whether the particle is located in

the possible contact range, as denoted by

$$d_f \leq r \quad (1)$$

where r indicates the radius of that particle, and the distance is determined by

$$d_f = (\mathbf{p} - \mathbf{v}_i) \cdot \mathbf{n} \quad (2)$$

where \mathbf{p} denotes position vector of particle centre, \mathbf{v}_i ($i=1, 2, 3, 4$) denote position vector of each vertex and \mathbf{n} is the normal of that facet, which is determined by

$$\mathbf{n} = \frac{\sum_{i=1}^4 \mathbf{e}_i \times \mathbf{e}_{i-1}}{|\sum_{i=1}^4 \mathbf{e}_i \times \mathbf{e}_{i-1}|} \quad (3)$$

where edge vector $\mathbf{e}_i = \mathbf{v}_{i+1} - \mathbf{v}_i$; \mathbf{e}_0 and \mathbf{v}_5 are equivalent to \mathbf{e}_4 and \mathbf{v}_1 , respectively.

Once Eq. (1) is confirmed to be true, the inside or outside examination of that particle centre to facet's edges is followed subsequently. The inside state is depended on the fulfilment of following criterion

$$\delta_i \leq tol \quad (4)$$

where tol is the tolerance and projection area δ_i is determined by

$$\delta_i = (\mathbf{e}_i \times (\mathbf{p} - \mathbf{v}_i)) \cdot \mathbf{n} \quad (5)$$

Once the criterion in Eq. (4) is passed for all edges of that facet, then PTF is confirmed to be true so that PTE and PTV are no longer necessary. The main task remained here is to get contact point \mathbf{c} on the facet, and this contact point is determined by vertex position vectors and related shape functions N_i

$$\mathbf{c} = \sum_{i=1}^4 N_i \cdot \mathbf{v}_i \quad (6)$$

With the projection area δ_i known, shape functions N_i on vertexes can be obtained by means of the method introduced in [13]

$$N_1 = \frac{\delta_2 \cdot \delta_3}{\delta}, N_2 = \frac{\delta_3 \cdot \delta_4}{\delta}, N_3 = \frac{\delta_4 \cdot \delta_1}{\delta}, N_4 = \frac{\delta_1 \cdot \delta_2}{\delta} \quad (7)$$

where base $\delta = (\delta_1 + \delta_3) \cdot (\delta_2 + \delta_4)$.

Conversely, once Eq. (4) is not fulfilled, then the particle centre must be outside of corresponding edge e_i . In this situation, PTF is failed and following inside-outside checks are terminated; however, this failure on PTF cannot exclude other possible contact conditions, such as PTE and PTV. Instead of PTF and making use of failed information passed down, PTE contact checking directly starts between the particle and the edge where PTF operation terminates.

2.2 PTE contact

Before PTE contact checking, the distance d_{ei} (Figure 2) between that particle centre and the edge e_i identified in PTF is required to be less than particle's radius, i.e.,

$$d_{ei} \leq r \quad (8)$$

where $d_{ei} = |\mathbf{p} - \mathbf{c}|$ and position vector \mathbf{c} of contact point is determined by

$$\mathbf{c} = \mathbf{v}_i + \left((\mathbf{p} - \mathbf{v}_i) \cdot \frac{\mathbf{e}_i}{|\mathbf{e}_i|} \right) \cdot \frac{\mathbf{e}_i}{|\mathbf{e}_i|} \quad (9)$$

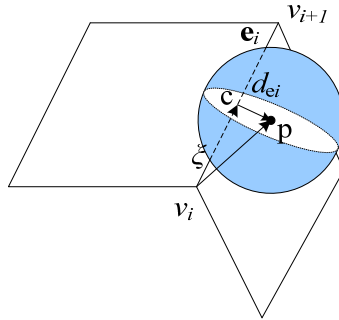


Figure 2: PTE contact checking

Once Eq. (8) fulfils, the second stage proceeds and its task is to examine whether contact point c is located on the edge or extension line. To do so, a coefficient ξ is define as

$$\xi = \frac{|\mathbf{c} - \mathbf{v}_i|}{|\mathbf{e}_i|} \quad (10)$$

and once

$$tol < \xi \leq 1 - tol \quad (11)$$

the contact point would locate in the range of edge e_i , then PTE is passed and PTV is no longer needed.

On the contrary, if $\xi \leq tol$ or $\xi > 1 - tol$, then contact point is located on the extension line along that edge and beyond vertex v_i or v_{i+1} , respectively. In this case, PTV, instead of PTE, needs to be further processed and the potential vertex can be simply determined using the value of ξ .

2.3 PTV contact

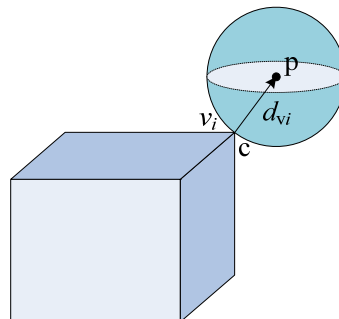


Figure 3: PTV contact checking

PTV is just to check the distance d_{vi} (Figure 3) between that particle centre and the related vertex identified in PTE and once it fulfils

$$d_{vi} \leq r \tag{12}$$

the PTV is passed and contact point c is coincident with that vertex v_i .

2.4 Implementation

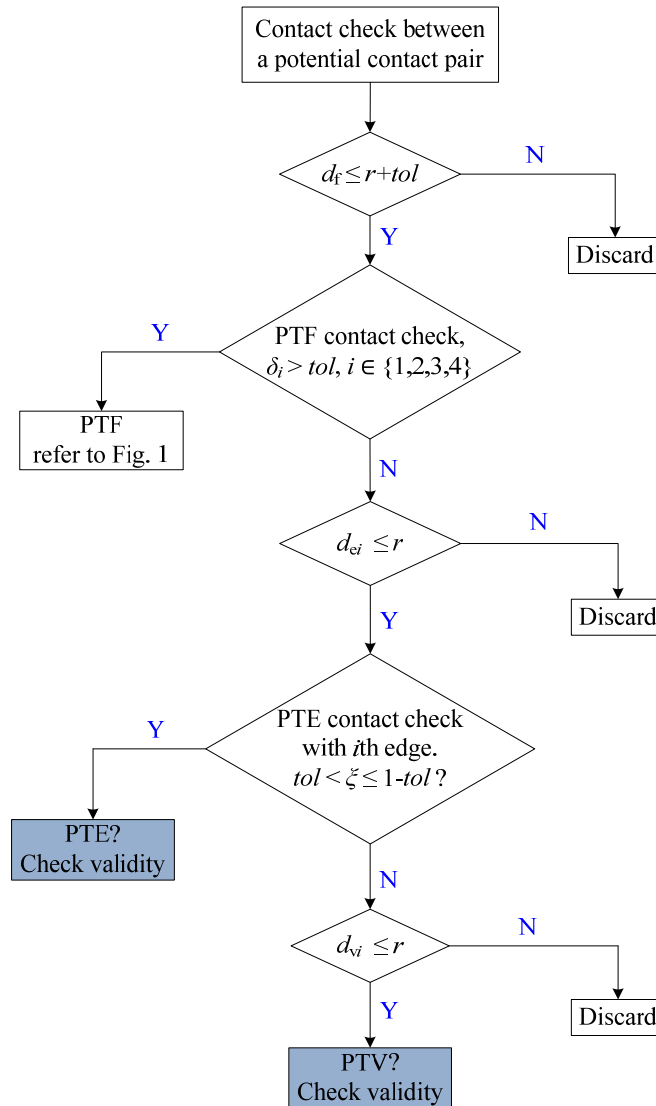


Figure 4: Flowchart of contact resolution implementation

The hierarchical searching strategy is inherently consistent and thus the implementation of proposed contact resolution algorithm is very straightforward. For each potential contact pair, contact resolution is processed from top (PTF) to bottom (PTV), and once an upper searching level is passed, the remaining searching levels no longer need to be processed. Inside each

level, a distance checking is initially conducted to exclude geometrically-impossible pairs. Once PTF or PTE is failed, the subsequent searching level of PTE or PTV can instantaneously commence because of the identified edge or vertex seamlessly passed down. The detailed implementation is shown in the flowchart of Figure 4.

Some special cases should be carefully examined to remove invalid contacts. For instance, a particle is in PTE contact with one facet and meanwhile confirmed to be in PTF contact with another facet (see Figure 5) or, in PTV contact with one facet and meanwhile in PTF (see Figure 6) or PTE (see Figure 7) contact with another facet. According to priority definition, so PTF (Figure 5), PTF (Figure 6) and PTE (Figure 7) should be approved for these three cases, respectively.

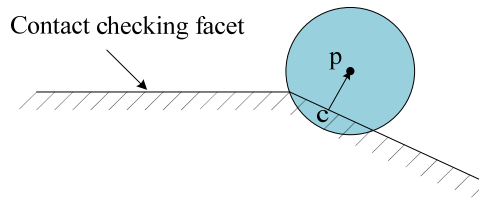


Figure 5: Invalid case of PTE: in PTF contact with another facet

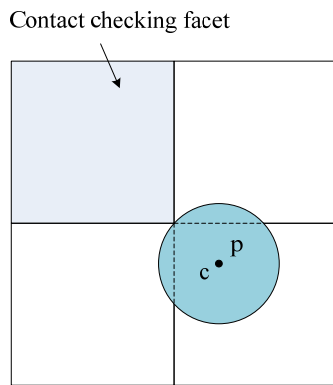


Figure 6: Invalid case of PTV: in PTF contact with another facet

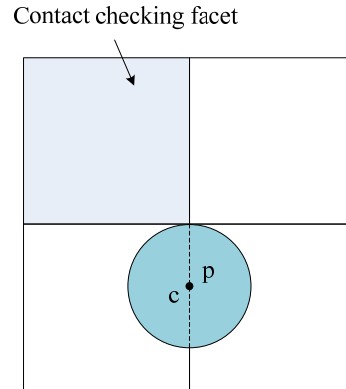


Figure 7: Invalid case of PTV: in PTE contact with another edge

3 CONTACT FORCE COMPUTATION

Hertz contact model [11] is used to compute contact force and is expressed as

$$\mathbf{F} = \alpha \cdot \frac{4}{3} \bar{E} r^{1/2} g^{3/2} \cdot \frac{(\mathbf{p} - \mathbf{c})}{|\mathbf{p} - \mathbf{c}|} \quad (13)$$

where α is penalty stiffness factor, g is inter-penetration as shown in Figure 8, and effective Young's modulus \bar{E} is determined by

$$\frac{1}{\bar{E}} = \frac{1 - \mu_1^2}{E_1} + \frac{1 - \mu_2^2}{E_2} \quad (14)$$

where μ_1 and μ_2 are Poisson ratios for the particle and facet, respectively. It is presumed that

inter-penetration is relatively small compared to particle radius, and to keep it small, the penalty stiffness factor is therefore used.

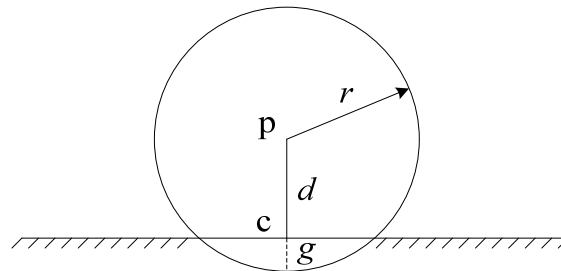


Figure 8: Schematic diagram of Hertz contact model

4 NUMERICAL EXAMPLE

A simple model is used to investigate contact behaviour of PTF, PTE and PTV. This model consists of a hexahedron finite element with the size of $1 \times 1 \times 1$ mm and a spherical discrete element with the radius of 0.5 mm. The material properties for both objects are: mass density 0.1 g/mm^3 , Young's modulus 1000 MPa and Poisson ratio 0. The initial velocity for discrete element is 10 m/s towards finite element and the penalty stiffness factors applied on these three contact cases are 10, 8 and 0.5, respectively. Rigid material model is selected for finite element and time step is set to be 1.0×10^{-3} ms.

PTF, PTE and PTV contact models are shown in Figure 9, Figure 11 and Figure 13, respectively, and the snapshots of their contact behaviour are displayed in Figure 10, Figure 12 and Figure 14, respectively. According to these figures, it is found that the contact problems of PTF, PTE and PTV can be correctly resolved.

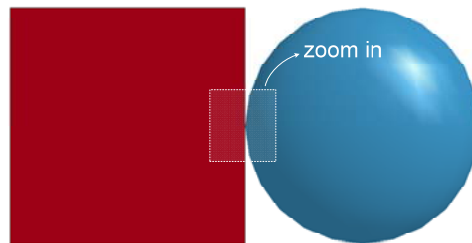


Figure 9: PTF contact model

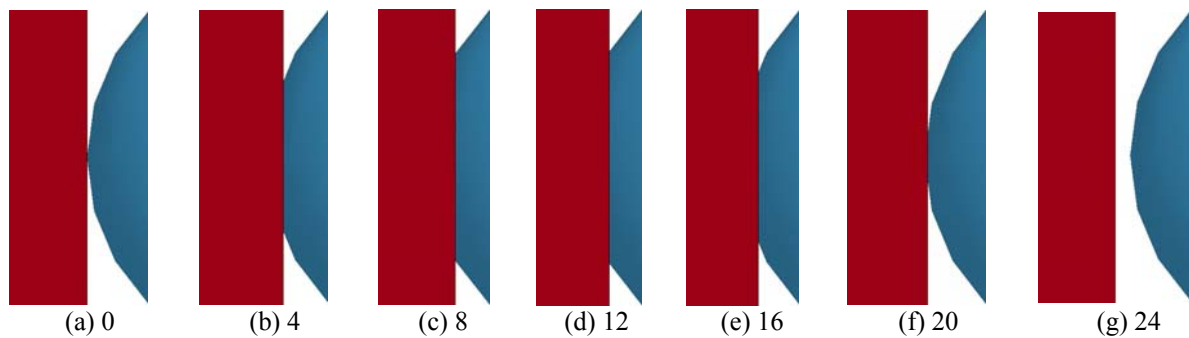


Figure 10: Snapshots of PTF contact (time: μs)

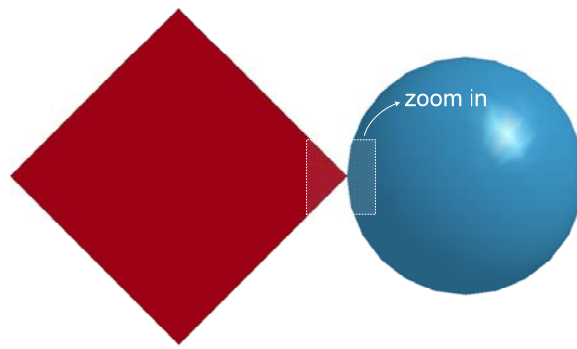


Figure 11: PTE contact model

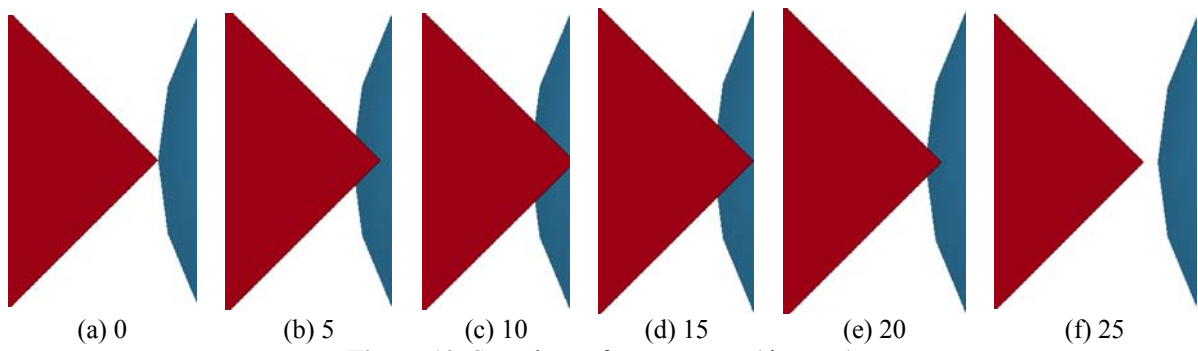


Figure 12: Snapshots of PTE contact (time: μs)

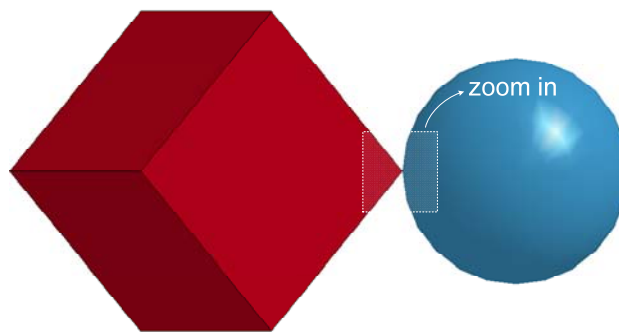


Figure 13: PTV contact model

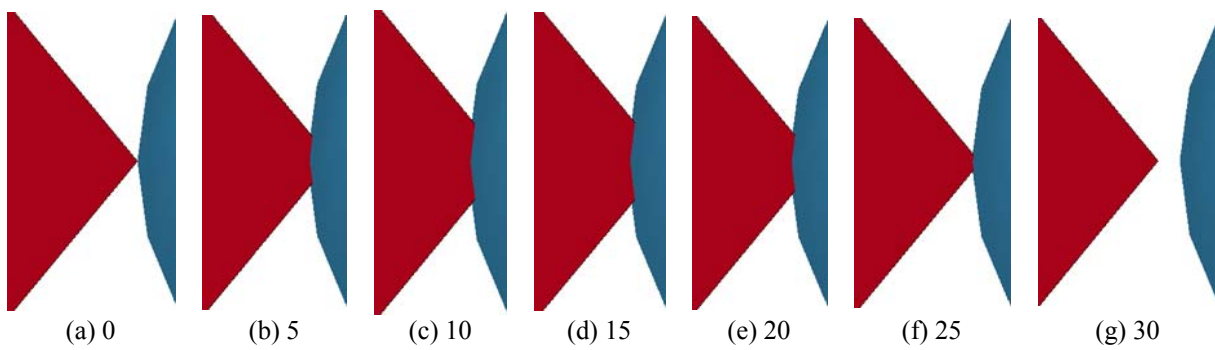


Figure 14: Snapshots of PTV contact (time: μs)

5 CONCLUSIONS

- An accurate and robust contact resolution algorithm for resolving contact problems in finite-discrete element system is developed.
- The contact resolution is robust by means of hierarchical searching strategy from PTF to PTE and to PTV.
- The hierarchical searching strategy is inherently consistent and its implementation is very straightforward.
- The invalid contacts are removed and the accuracy of algorithm can be better guaranteed.

ACKNOWLEDGEMENT

The in-house code CDFP from Prof. Zang's group and financial support from the China Scholarship Council and UNSW Canberra awarded to Hu Chen are gratefully acknowledged.

REFERENCES

- [1] Munjiza, A. *The combined finite-discrete element method*. West Sussex: John Wiley & Sons, (2004).
- [2] Nakashima, H. and Oida, A. Algorithm and implementation of soil-tire contact analysis code based on dynamic FE-DE method. *J. Terramech.* (2004) **41**:127-137.
- [3] Zang, M. and Zhao, C. Numerical simulation of rigid wheel running behavior on sand terrain. In *APCOM & ISCM*, (2013).
- [4] Lei, Z. and Zang, M. An approach to combining 3D discrete and finite element methods based on penalty function method. *Comput. Mech.* (2010) **46**:609-619.
- [5] Kodam, M., Bharadwaj, R., et al. Force model considerations for glued-sphere discrete element method simulations. *Chem. Engng. Sci.* (2009) **64**:3466-3475.
- [6] Dang, H.K. and Meguid, M.A. An efficient finite–discrete element method for quasi-static nonlinear soil–structure interaction problems. *Int. J. Num. Anal. Met.* (2013) **37**:130-149.
- [7] Kremmer, M. and Favier, J.F. A method for representing boundaries in discrete element modelling—part I: Geometry and contact detection. *Int. J. Num. Meth Engng.* (2001) **51**:1407-1421.
- [8] Zang, M., Gao, W., and Lei, Z. A contact algorithm for 3D discrete and finite element contact problems based on penalty function method. *Comput. Mech.* (2011) **48**:541-550.
- [9] Su, J., Gu, Z., and Xu, X.Y. Discrete element simulation of particle flow in arbitrarily complex geometries. *Chem. Engng. Sci.* (2011) **66**:6069-6088.
- [10] Hu, L., Hu, G.M., et al. A new algorithm for contact detection between spherical particle and triangulated mesh boundary in discrete element method simulations. *Int. J. Num. Meth Engng.* (2013) **94**:787-804.
- [11] Johnson, K.L. *Contact mechanics*. Cambridge: Cambridge University Press, (1987).
- [12] Wang, S.P. and Nakamachi, E. The inside–outside contact search algorithm for finite element analysis. *Int. J. Num. Meth Engng.* (1997) **40**:3665-3685.
- [13] Zhong, Z.H. *Finite element procedures for contact-impact problems*. New York: Oxford University Press, (1993).